Journal of Engineering Physics and Thermophysics, Vol. 68, No. 4, 1995

QUASI-EQUILIBRIUM STATES OF A LOW-TEMPERATURE AIR PLASMA OF REDUCED DENSITY

L. N. Panasenko, G. S. Romanov,
Yu. A. Stankevich, and K. L. Stepanov

UDC 533.95:537.56

Quasistationary states of an air plasma of reduced density are considered on the basis of equations of chemical and ionization kinetics. The component composition and thermodynamic quantities are compared with data obtained in an equilibrium approximation.

Introduction. The assumption of total thermodynamic equilibrium, within the framework of which most data on thermodynamic and optical properties of plasma have been obtained, is known to be limited both for a multiply charged high-temperature plasma and for a low-temperature plasma of reduced density. One of the mechanisms that lead to a deviation from equilibrium is radiative transitions, not compensated by the corresponding processes of radiation absorption. In a multiply charged plasma where the ratio of radiation and collisional transition rates is proportional to the ratio Z^7/N_e, thermodynamic equilibrium is only possible at high densities and in the general case the state is described by a radiation-collisional model [1-3]. Approximations of thermodynamic and coronal equilibrium are the limiting cases of the latter [4, 5]. In a low-temperature plasma the processes of radiative molecular recombination and atomic photorecombination become substantial with a decrease in density. The medium often proves to be transparent to the intrinsic radiation and the time in which the quasistationary state is established is noticeably smaller than the characteristic time of plasma evolution. In this case we can speak of quasi-equilibrium states that are governed by two variables, for example, temperature and density, but, unlike the states of thermodynamic equilibrium, depend on the entire set of collisional and radiation processes.

Model of Quasi-Equilibrium. The kinetic model considered in this work includes 48 reactions between the following 18 components: N_2, O_2, NO, N, O, Ar, N_2^+, O_2^+, NO^+, N^+, O^+, Ar^+, e, N^{+2}, O^{+2}, Ar^{+2}, N^{+3}, and O^{+3}. The reactions included in the model are listed below:

1. $N_2 + O_2 \Leftrightarrow N + N + O_2$
2. $N_2 + N \Leftrightarrow N + N + N$
3. $N_2 + N_2 \Leftrightarrow N + N + N_2$
4. $N_2 + NO \Leftrightarrow N + N + NO$
5. $N_2 + O \Leftrightarrow N + N + O$
6. $O_2 + N_2 \Leftrightarrow O + O + N_2$
7. $O_2 + O \Leftrightarrow O + O + O$
8. $O_2 + O_2 \Leftrightarrow O + O + O_2$
9. $O_2 + NO \Leftrightarrow O + O + NO$
10. $O_2 + N \Leftrightarrow O + O + N$
11. $NO + N \Leftrightarrow N + O + N$
12. $NO + NO \Leftrightarrow N + O + NO$
13. $NO + N_2 \Leftrightarrow N + O + N_2$
14. $NO + O_2 \Leftrightarrow N + O + O_2$
15. $NO + O \Leftrightarrow N + O + O$
16. $O + N_2 \Leftrightarrow NO + N$
17. $NO + O \Leftrightarrow N + O_2$
25. $O + NO^+ \times N^+ + O_2$
26. $NO^+ + NO \Leftrightarrow O_2^+ + N_2$
27. $N + O \Leftrightarrow NO^+ + e$
28. $O + O \Leftrightarrow O_2^+ + e$
29. $N + N \Leftrightarrow N_2^+ + e$
30. $N + e \Leftrightarrow N^+ + e + e$
31. $O + e \Leftrightarrow O^+ + e + e$
32. $Ar^+ e \Leftrightarrow Ar^+ + e + e$
33. $N^+ + e \Leftrightarrow N^{+2} + e + e$
34. $O^+ + e \Leftrightarrow O^{+2} + e + e$
35. $Ar^+ + e \Leftrightarrow Ar^{+2} + e + e$
36. $N^{+2} + e \Leftrightarrow N^{+3} + e + e$
37. $O^{+2} + e \Leftrightarrow O^{+3} + e + e$
38. $N + N \Leftrightarrow N_2 + h\nu$
39. $O + O \Leftrightarrow O_2 + h\nu$
40. $N + O \Leftrightarrow NO + h\nu$
41. $N^+ + e \Leftrightarrow N + h\nu$

Academic Scientific Complex "A. V. Luikov Institute of Heat and Mass Transfer of the Academy of Sciences of Belarus," Minsk. Translated from Inzhenerno-Fizicheskii Zhurnal, Vol. 68, No. 4, pp. 569-575, July-August, 1995. Original article submitted December 28, 1993.

 1062-0125/95/6804-0464$12.50

18. $O + O_2^+ \Leftrightarrow O^+ + O_2$
19. $O^+ + N_2 \Leftrightarrow O + N_2^+$
20. $O + NO^+ \Leftrightarrow O^+ + NO$
21. $N + O_2^+ \Leftrightarrow N^+ + O_2$
22. $N^+ + N_2 \Leftrightarrow N + N^+_2$
23. $O_2 + NO^+ \Leftrightarrow O_2^+ + NO$
24. $N + NO^+ \Leftrightarrow N_2^+ + O$
42. $O^+ + e \Leftrightarrow N + h\nu$
43. $Ar^+ + e \Leftrightarrow Ar + h\nu$
44. $N^{+2} + e \Leftrightarrow N^+ + h\nu$
45. $O^{+2} + e \Leftrightarrow O^+ + h\nu$
46. $Ar^{+2} + e \Leftrightarrow A\rho^+ + h\nu$
47. $N^{+3} + e \Leftrightarrow N^{+2} + h\nu$
48. $O^{+3} + e \Leftrightarrow O^{+2} + h\nu$

These are reactions of dissociation and three-particle association of N_2, O_2, and NO molecules 1-15, bimolecular reactions 16-17, recharging reactions and ion-molecular reactions 18-26, associative ionization processes and reverse processes of dissociative recombination 27-29, processes of electron impact ionization and reverse processes of triple recombination 30-37, reactions of molecular photoassociation 38-40, and reactions of ionic photorecombination 41-48.

The system of kinetic equations that describes the dependences of the plasma composition on temperature and density appears as

$$\frac{dN_i}{dt} = \sum_{k=1}^{M} \left[V_k^+ \prod_s N_s^{\alpha_{si}^+} - V_k^- \prod_s N_s^{\alpha_{si}^-} \right] (\alpha_{si}^+ - \alpha_{si}^-), \tag{1}$$

here $k = 1,..., M$ is the number of reactions that result in the formation or elimination of the ith component; $V_R^{\pm}$ is the rate of these reactions; $\alpha_{si}^{\pm}$ is their stoichiometric coefficients; under the symbol $\prod$ are the concentrations of the interacting components. The states of quasi equilibrium correspond to stationary solutions to the system (1).

The constants of direct and reverse reaction rates (1-48) (see above) were chosen according to the recommendations of [6-9] and are given in Table 1. The rates of bimolecular reactions have here dimensions of cm^3/sec, reactions with the involvement of three particles cm^6/sec, and the temperature eV. We point out that the rates of direct ion-molecular reactions 25-26 were calculated in terms of the rates of reverse reactions and equilibrium constants*.

The rates of the processes of impact ionization and atomic and ionic recombination are calculated within the framework of [2, 4]. We can tabulate them depending on the temperature of electrons and their concentration, they being dependent in a complex manner on the atomic characteristics of the particle and governed by a large number of elementary acts (excitation and quenching of the given electron state, ionization, recombination and spontaneous radiation disintegration of the level, etc.). Thus, the calculated ionization rate takes account of stepwise ionization processes that become predominant as the temperature and density increase, and the recombination rate includes both the processes of triple recombination at relatively high electron concentrations and low temperatures (the recombination frequency being proportional to $i^3 N_e^2 T^{-9/2}$) and those of photorecombination of which the dependence $N_e/\sqrt{T}$ is typical. In this work, in calculating the rates of electron impact ionization we used a simpler approximation [1] that assumes ionization from the basic particle states. The constants of triple recombination rates were prescribed in the Gurevich-Pitaevski approximation.

Radiative atomic recombination with the formation of molecules 38-40 was described in the form proposed in [10].** The rates of photorecombination reactions 41-48 were determined according to [1]:

$$V_i = 10^{-14} \left(\frac{I_i}{13.6} \right)^{1/2} \left(\frac{I_i}{T} \right)^{1/2} \frac{B_i}{1 + T I_i^{-1} x_i}, \tag{2}$$

where I_i is the ionization potentials; B_i and x_i are the quantities tabulated in [1].

---

* q_{25} and q_{26} are equal to the ratios of electron and vibrational statistical sums: $q_{25} = \sum^e_{O_2} \sum^v_{O_2} \sum^e_{N^+} / (\sum^e_{NO^+} \sum^e_{NO^+} \sum^2_{O})$, $q_{26} = \sum^e_{O_2^+} \sum^v_{O_2^+} \sum^e_{N_2^+} \sum^v_{N_2^+} / (\sum^e_{NO} \sum^v_{NO} \sum^e_{NO^+} \sum^v_{NO^+})$, and rotational statistical sums are included in the coefficients.

** The expression for G_0 is taken from [10].

TABLE 1. Reaction Rates

Number of reaction	Direct reaction V	Reverse reaction $\tilde{V}$
1	$5{,}31\cdot10^{-8}e^{-9{,}76/T}(1-e^{-0{,}292/T})$; $\frac{2{,}28\cdot10^{-9}}{T^{3{,}5}}e^{-9{,}76/T}$, $T\geq 0{,}52$;	$10^{-34}\max(8{,}3e^{0{,}043/T};\ 19)$ V_1/K_p, $T\geq 0{,}543$
2	$2{,}2V_1$; $4{,}27TV_1$, $T\geq 0{,}52$;	$6\tilde{V}_1$
3	V_1	$\tilde{V}_1$
4	V_1	$\tilde{V}_1$
5	V_2	$\tilde{V}_2$
6	$9{,}27\cdot10^{-9}e^{-5{,}12/T}(1-e^{-0{,}196/T})$; $\frac{2{,}80\cdot10^{-10}}{T^{2{,}5}}e^{-5{,}12/T}$, $T\geq 0{,}345$;	$1{,}66\cdot10^{-10}e^{0{,}062/T}$ V_6/K_p, $T\geq 0{,}043$
7	$1{,}32\cdot10^{-7}e^{-5{,}12/T}(1-e^{-0{,}196/T})$; $4\cdot10^{-9}T^{-2{,}5}e^{-5{,}12/T}$, $T\geq 0{,}345$;	$2{,}53\cdot10^{-33}T^{-0{,}63}$ V_7/K_p, $T\geq 0{,}345$
8	$4V_6$	$0{,}278\tilde{V}_7$; V_8/K_p, $T\geq 0{,}345$
9	V_6	$0{,}25\tilde{V}_8$
10	V_6	$\tilde{V}_9$
11	$2\cdot10^{-7}(1-e^{-0{,}236/T})e^{-6{,}51/T}$;	$1{,}64\cdot10^{-33}/\sqrt{T}$
12	V_{11}	$\tilde{V}_{11}$
13	$0{,}05V_{11}$	$\tilde{V}_{11}$
14	V_{13}	$\tilde{V}_{11}$
15	V_{11}	$\tilde{V}_{11}$
16	$1{,}26\cdot10^{-10}e^{-3{,}26/T}$;	$10^{-11}\max(3{,}11;\ 11{,}3\sqrt{T})$
17	$2{,}9\cdot10^{-11}Te^{-1{,}681/T}$;	$1{,}23\cdot10^{-10}Te^{-0{,}272/T}$;
18	$1{,}46\cdot10^{-12}T^{-0{,}52}e^{-1{,}617/T}$;	$1{,}46\cdot10^{-12}T^{-0{,}52}$
19	$1{,}47\cdot10^{-10}T^{-0{,}21}e^{-1{,}914/T}$;	$2{,}48\cdot10^{-12}T^{-0{,}21}$
20	$5{,}02\cdot10^{-11}T^{-0{,}01}e^{-4{,}397/T}$;	$2{,}16\cdot10^{-11}T^{0{,}01}$
21	$8{,}78\cdot10^{-13}T^{-0{,}52}e^{-1{,}603/T}$;	$1{,}53\cdot10^{-12}T^{-0{,}7}$
22	$3{,}04\cdot10^{-12}T^{-0{,}18}e^{-1{,}043/T}$;	$1{,}83\cdot10^{-14}T^{-0{,}52}$
23	$3{,}48\cdot10^{-9}T^{-0{,}17}e^{-2{,}793/T}$;	$9{,}11\cdot10^{-10}T^{-0{,}17}$
24	$1{,}19\cdot10^{-9}T^{-0{,}4}e^{-3{,}06/T}$;	$1{,}73\cdot10^{-10}T^{0{,}4}$
25	$2{,}18\cdot10^{-10}q_{25}e^{-6{,}656/T}$;	$3{,}5\cdot10^{-10}$
26	$2{,}53\cdot10^{-18}q_{26}e^{-0{,}933/T}$;	10^{-17}
27	$8{,}1\cdot10^{-12}T^{0{,}37}e^{-2{,}761/T}$;	$2{,}84\cdot10^{-8}T^{-0{,}75}$
28	$6{,}28\cdot10^{-11}T^{0{,}49}e^{-6{,}948/T}$;	$1{,}75\cdot10^{-8}T^{-0{,}66}$
29	$4{,}0\cdot10^{-10}T^{0{,}77}e^{-5{,}819/T}$;	$4{,}33\cdot10^{-8}T^{-0{,}39}$
30	$3{,}11\cdot10^{-7}\,Te^{-14{,}54/T}(14{,}54+0{,}21T)^{-1}\times$ $\times(14{,}54+T)^{-1/2}$	$5{,}4\cdot10^{-27}T^{-9/2}$
31	$3{,}44\cdot10^{-7}Te^{-13{,}614/T}(13{,}61+0{,}22T)^{-1}\times$ $\times(13{,}61+T)^{-1/2}$	$\tilde{V}_{30}$
32	$6{,}37\cdot10^{-7}Te^{-15{,}76/T}(15{,}76+T)^{-3/2}$	$\tilde{V}_{30}$
33	$7{,}74\cdot10^{-8}\sqrt{T}\,e^{-29{,}61/T}(29{,}6+0{,}5T)^{-1}$	$8\tilde{V}_{30}$
34	$1{,}44\cdot10^{-7}\sqrt{T}\,e^{-35{,}15/T}(35{,}15+0{,}42T)^{-1}$	$\tilde{V}_{33}$
35	$3{,}03\cdot10^{-7}\sqrt{T}\,e^{-27{,}63/T}(27{,}6+T)^{-1}$	$\tilde{V}_{33}$
36	$9{,}35\cdot10^{-8}\sqrt{T}\,e^{-47{,}426/T}\,(47{,}426+0{,}65T)^{-1}$	$27\tilde{V}_{30}$
37	$1{,}46\cdot10^{-7}\sqrt{T}\,e^{-54{,}934/T}\,(54{,}934+0{,}57T)^{-1}$	$\tilde{V}_{36}$
38	$5{,}98\cdot10^{-21}\sqrt{T}\,e^{-2{,}38/T}$	
39	$4{,}9\cdot10^{-16}\sqrt{T}\,G_0$	
40	$1{,}59\cdot10^{-18}/\sqrt{T}$	

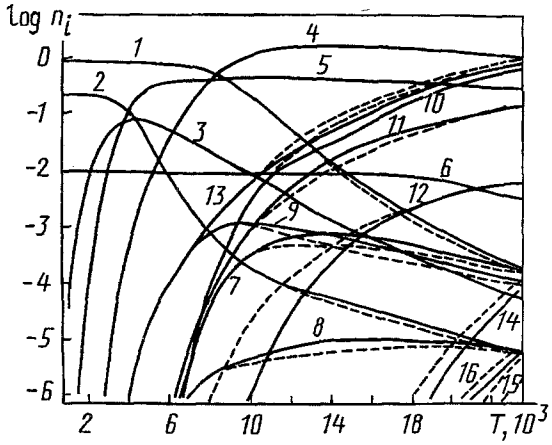

Fig. 1. Composition of the air plasma of normal density $\rho_0 = 1.29 \cdot 10^{-3}$ g/cm^3. The solid lines are the quasistationary distribution, the dashed ones are the thermodynamic equilibrium: 1) N_2; 2) O_2; 3) NO; 4) N; 5) O; 6) Ar; 7) N_2^+; 8) O_2^+; 9) NO^+; 10) N^+; 11) O^+; 12) Ar^+; 13) e; 14) N^{+2}; 15) O^{+2}; 16) Ar^{+2}; 17) N^{+3}; 18) O^3. (Curves 17 and 18 are not drawn so as not to increase the field of the figure). T, K.

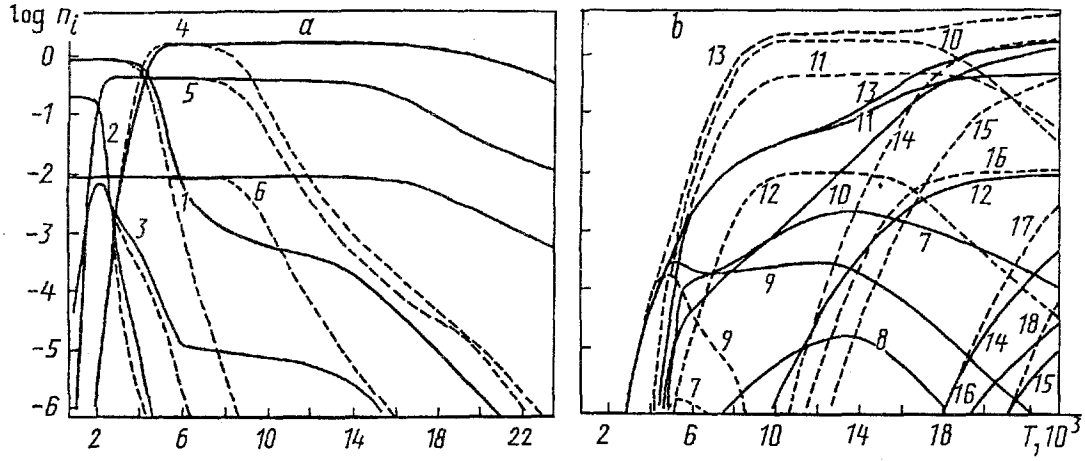

Fig. 2. Composition of the air plasma with the relative density $\rho/\rho_0 = 10^{-6}$: a) neutral components; 6) charged ones. The denotation is the same as in Fig. 1.

To obtain the quasi-stationary state, we need to find the asymptotic form of the solution (1) as $t \to \infty$, i.e., to solve, in fact, the system of nonlinear equations that make the right-hand sides vanish. This system of equations is rigid since the differences in the rates of the processes can attain many orders. Correspondingly the vector of the solution contains components that differ in order of magnitude. The combination of the relaxation method, whose most important element is normalization at each step of the solution, with the conservation laws and a modified Newton method proved to be an efficient method for solving this problem [11].

Discussion of Results. We investigated the states of quasi-equilibrium for the air plasma (with the volume content of the components N_2 0.7812, O_2 0.2095, and Ar 0.0093) in the $0.1 < T < 2$ eV temperature and $10^{-9} < \rho < 10^{-3}$ g/cm^3 density range. Calculations by this model showed that practically in the entire region of parameters in question the solution is different from the thermodynamically equilibrium one. Figure 1 compares the composition of air of normal density with the equilibrium calculations [12]. The concentrations of the particles are normalized to their total number for $T \to 0$ and the given density. In this variant, to elucidate the role of reactions 38-48 in the total balance, we calculated all reverse rates of collision $\widetilde{V}$ in terms of equilibrium constants. At the given density, taking into account photoprocesses leads to corrections to the equilibrium distribution: double-charged ions occur at higher temperatures, atomic photoassociation increases the concentration of molecules. At

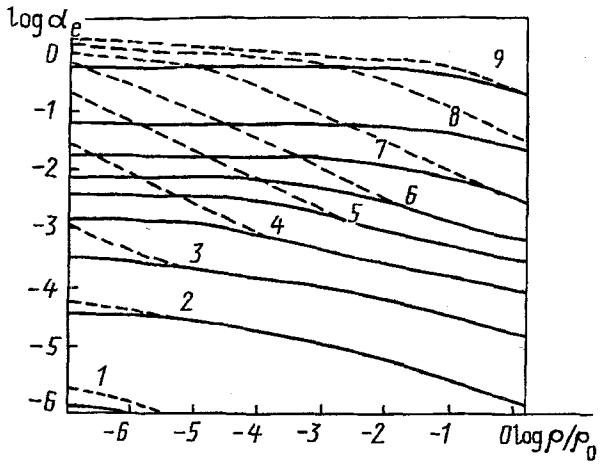

Fig. 3. Degree of ionization as a function of temperature and density of the plasma: 1) $T = 3 \cdot 10^3$; 2) 4; 3) 5; 4) 6; 5) 7; 6) 8; 7) 10; 8) 14; 9) $20 \cdot 10^3$ K.

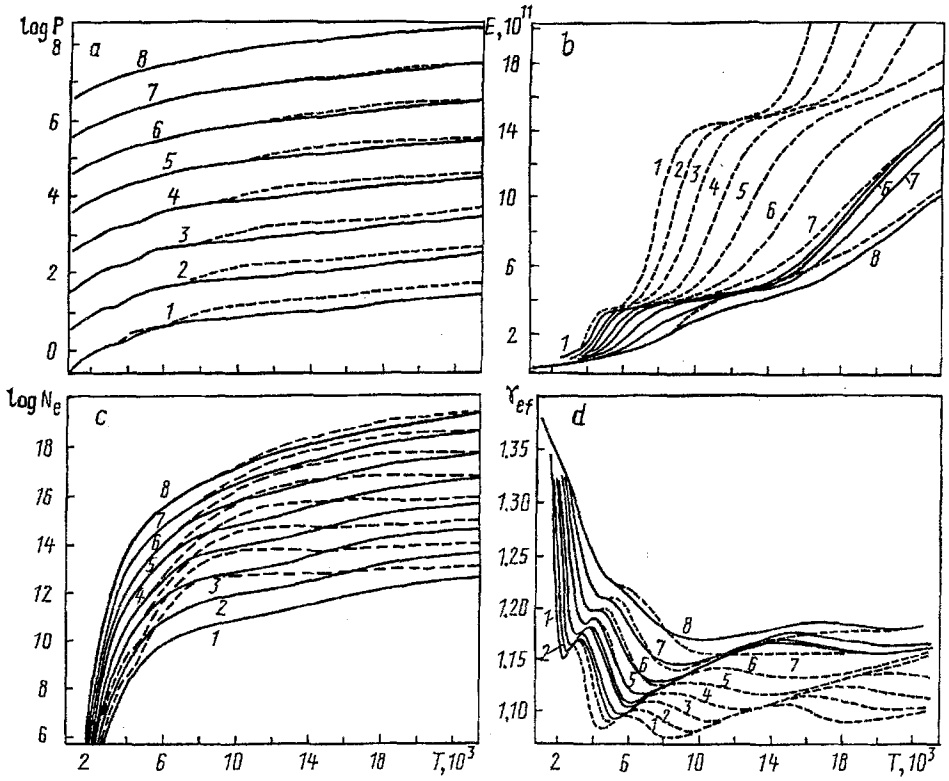

Fig. 4. Pressure (a), specific energy (b), electron concentration (c), and adiabatic exponent (d) vs temperature and density: 1) $\rho/\rho_0 = 10^{-7}$, ... 8) $\rho/\rho_0 = 1$. log P, erg/cm^3; E, 10^{11} erg/g; log N_e, cm^3

the same time the concentration of single-charged and molecular ions, because of a high recharging rate as compared to photorecombination, remains practically unchanged for temperatures below 104 K but changes noticeably in the region of higher temperatures.

Results of the calculations that refer to a low density region are given in Fig. 2. Here all the reaction rates were prescribed according to the table. In this case, the substantial difference from the equilibrium results is evident not only for small components but also for the leading ones. The electron concentration decreases to an order of magnitude and lower as compared to the equilibrium one at a temperature above $3 \cdot 10^3$ K; the neutral component (N_2, N, O, Ar) exists in considerable amounts up to very high temperatures; the molecular ion concentration proves to be many orders of magnitude higher than the equilibrium one.

The transition of the quasi-equilibrium state from the thermodynamic equilibrium state to the state of coronal equilibrium that is realized in the limiting case of low densities is quite evident from the dependence of the degree of ionization for the plasma on its density (the degree of ionization is determined as the ratio of the electron concentration to the overall concentration of the remaining particles). Its dependence on density is shown in Fig. 3 for the set of temperatures. It is evident that as the temperature increases this transition takes place at progressively higher densities. We point out that the coronal limit corresponds to a density-independent degree of ionization.

Knowledge of the component composition permits determination of its macroscopic characteristics. Figure 4 gives the results of calculating the pressure, specific internal energy, electron concentration, and the effective adiabatic exponent; the analogous equilibrium values are shown dashed here. It is noteworthy that in calculating the thermodynamic quantities we assumed the Boltzmann population of excited levels. In view of the small contribution of particle excitation energy to the total energy, this assumption is quite acceptable, however, to determine the optical properties, a detailed description of the kinetics of population of the excited states is required. This approach is described in [5] in a multiply charged air plasma. It is much more difficult to perform the analogous analysis at low temperatures due to the large number of degrees of freedom.

In solving Eqs. (1) we found the times of establishment of the quasi equilibrium τ_p. They, as is known, depend rather weakly on the initial state of the system and are governed by the largest relaxation time of components in the plasma. For a normal density, as the temperature increases from $3\cdot10^3$ to $2\cdot10^4$ K, τ_p changes in the $10^{-2}-10^{-8}$ sec interval. At smaller temperatures the probabilities of nonelastic processes drop exponentially and τ_p increases correspondingly. The approximate dependence of τ_p on density appears in the considered range of conditions as $\tau_p \sim \rho^{-s}$, where $s \simeq 0.7-1$.

NOTATION

ρ, density; T, temperature; P, pressure; E, specific internal energy; γ_{ef}, effective adiabatic exponent; N_i, particle concentration; Σ_i, statistical sum; I_i, ionization potential; V_i and $\widetilde{V}_i$, direct and reverse reaction rates.

REFERENCES

1. L. A. Vainshtein, I. I. Sobel'man, and E. A. Yukov, Atom Excitation and Spectral Line Broadening [in Russian], Moscow (1979).
2. V. I. Derzhiev, A. G. Zhidkov, and S. I. Yakovenko, Ion Radiation in a Nonequilibrium Dense Plasma [in Russian], Moscow (1986).
3. G. S. Romanov, K. L. Stepanov, L. K. Stanchits, and A. V. Teterev, Dokl. Akad. Nauk BSSR, **29**, No. 11, 1094-1097 (1985).
4. B. N. Bazylev, F. N. Borovick, G. S. Romanov, et al., Laser and Particle Beams, **6**, No. 4, 709-721 (1988).
5. G. S. Romanov, L. K. Stanchits, and K. L. Stepanov, Zh. Prikl. Spektr., **54**, No. 5, 825-832 (1991).
6. O. E. Krivonosova, S. A. Losev, V. P. Nalivaiko, et al., Khim. Plazmy, Issue 14, 3-31 (1988).
7. A. Kh. Mnatsakanyan and G. V. Naidis, Khim. Plazmy, Issue 14, 227-255 (1988).
8. L. M. Biberman, V. S. Vorob'yov, and I. T. Yakubov, Kinetics of Nonequilibrium Low Temperature Plasmas [in Russian], Moscow (1982).
9. E. V. Stupochenko, S. A. Losev, and A. I. Osipov, Relaxation Processes in Shock Waves [in Russian], Moscow (1982).
10. B. V. Zamyshlyaev, E. L. Stupitskii, A. G. Guz', and V. N. Zhukov, Composition and Thermodynamic Functions of Plasma [in Russian], Moscow (1984).
11. J. Dennis and R. Schnabel, Numerical Methods of Unconstrained Optimization and Solution for Nonlinear Equations [Russian translation], Moscow (1988).
12. G. S. Romanov, Yu. A. Stankevich, L. K. Stanchits, et al., Thermodynamical Properties, Spectral and Mean Absorption Coefficients of Gases in a Wide Range of Parameters, Minsk (1993), (Preprint/ITMO, 6).